

Electronic Supplementary Information

Section S1: Materials and Analytical Techniques

Materials. Terephthalic acid (H_2BDC , 98% purity), zirconyl chloride octahydrate ($\text{ZrOCl}_2 \cdot 8\text{H}_2\text{O}$, 98%), and zirconium(IV) chloride (ZrCl_4 , 99.5%) were purchased from Sigma-Aldrich. Vitamin B12 (98%) was purchased from Sigma-Aldrich. N, N-dimethylformamide (DMF, 99.9% extra dry grade) and formic acid (HCOOH , 97%) were obtained from Daejung Chemical Company.

Analytical techniques. Powder X-ray diffraction (PXRD) patterns of the UiO-66 xerogel monoliths were collected using a RIGAKU MiniFlex600 diffractometer. Fourier transform infrared (FT-IR) spectra were measured using a PerkinElmer FT-IR spectrometer (Frontier model) using the ATR protocol. The morphology of the UiO-66 gels was determined by scanning electron microscopy (SEM; Leo-Supra 55, Carl Zeiss STM). The N_2 adsorption isotherms of the UiO-66 xerogel monoliths were measured at 77 K using BELSORP-max. The surface area of the samples was calculated from the N_2 isotherms using the Brunauer–Emmett–Teller (BET) method. The mesopore size of the xerogel monoliths was calculated from the N_2 desorption isotherms using the Barrett–Joyner–Halenda (BJH) method.

The electrochemical catalysis characterizations of the UiO-66 xerogel monoliths and $\text{VB}@\text{UiO-66}_m$ were performed using an Autolab electrochemical workstation (Metrohm, Netherlands). The three-electrode electrochemical cell configuration was used for the electrochemical hydrogen evolution reaction (HER) measurements under H_2 bubbling. A glassy carbon electrode (GCE, area = 0.196 cm^2) was used as the working electrode, and a platinum plate and saturated calomel electrode (SCE) were used as the counter and reference electrodes, respectively, in an H_2 -saturated 1-M HCl electrolyte. Voltages were converted from the SCE to the reversible hydrogen electrode (RHE) using the equation $E_{\text{RHE}} = E_{\text{SCE}} + (-0.2625)$, where E_{RHE} denotes the potential vs. RHE, E_{SCE} denotes the potential vs. SCE, and -0.2625 V is the voltage from the calibration of the H_2 -saturated 1-M HCl electrolyte using the three-electrode setup at $i = 0$ (Pt foil: working electrodes; carbon rod: counter electrode; calomel: reference electrode).¹ The Tafel plots were obtained using the equation $\eta = a + b \times \log|j|$, where a represents the intercept, b represents the slope, and j represents the

current density. Chronoamperometry was then performed at a potential of 57.5 mV (vs. RHE) for the stability test.

The TOF was calculated using the following equation:

$$\text{TOF} = j \times N_A / (F \times n \times \Gamma)$$

where j = current density (mA cm^{-2}), N_A = the Avogadro constant, F = the Faraday constant, $n = 2$, which is the number of electrons transferred to generate one molecule of the product, and Γ = number of active sites catalyzing the reaction (cm^{-2}).²

Section S2: Experiential Procedure

Synthesis of UiO-66 gels and xerogel monoliths. A mixture of $\text{ZrOCl}_2 \cdot 8\text{H}_2\text{O}$ (1 g, 3.1 mmol) and H_2BDC (1 g, 6 mmol) was dissolved in 150 mL of DMF. Different amounts of formic acid were added to the solution. The reaction mixture was heated at 120°C in an isothermal oven for 18 h and then cooled to room temperature. The gel-based products were collected by centrifugation (10 min, 8000 rpm, two separate centrifugation tubes of ~ 30 ml for each) and exchanged with DMF (3×25 ml, 2 days). Solvent exchange with ethanol (EtOH) (3×35 ml, 2 days) was performed. After solvent exchange, the gels were aged under high-speed centrifugation at 10°C (10 minutes, 12000 rpm) to obtain the post-aged gels, which were then filled in the cylinder pump (3 ml, nozzle size ~ 1.8 mm). The post-aged gels were gradually pumped onto a supporting paper surface to afford rod-shaped monoliths. The post-shaping monoliths were then dried under vacuum at room temperature for 1 h to obtain xerogel monoliths of different mesopore sizes, denoted as $\text{UiO-66}_m@x$, where x (4, 6, 8, and 10 ml) represents the amount of the HCOOH modulator used. The samples were then activated under a dynamic vacuum at 150°C for 12 h before N_2 adsorption at 77 K.

Synthesis of UiO-66 powder. A mixture of ZrCl_4 (1 g, 4.29 mmol) and H_2BDC (1 g, 6 mmol) was dissolved in 200 mL of DMF. Subsequently, acetic acid (8 ml) was added to the solution. The reaction mixture was heated at 120°C in an isothermal oven for 18 h and then cooled to room temperature. The products were collected by centrifugation, solvent-exchanged, and activated using the same procedure as that for the gel-based samples.

Adsorption of vitamin B12. 5 mg of $\text{UiO-66}_m@x$ (ground samples with monolith sizes ranging from 0.1 to 0.3 mm) or UiO-66 powder were weighed in a vial. Subsequently, a 1-ml EtOH solution of VB at different initial concentrations ($C_0 = 0.8, 1.2, 1.6, 2, 2.4,$ and 2.8 g L^{-1}) was added. The vial was then shaken at 200 rpm and 30°C for 20 h. At the endpoint, 0.2 ml of the solution was withdrawn and diluted in 1.8 ml of EtOH. The amount of adsorbed VB in the xerogel monoliths was calculated by VB titration of the EtOH solution by ultraviolet–visible (UV–Vis) spectroscopy. The EtOH solutions were then decanted, and the solid samples ($\text{VB} \subset \text{UiO-66}_m@x$) were dried under vacuum at 50°C .

Mesopore Shrinkage. Water (15 μL) was added to $\text{VB}\subset\text{UiO-66}_m@x$. The samples were then dried at 50°C for 30 min under vacuum to obtain $\text{VB}\subset\text{UiO-66}_m@x\text{S}$ in the shrinkage form.

Desorption of VB. Water (10 ml) was added to the vials containing $\text{VB}\subset\text{UiO-66}_m@x$ (5 mg based on $\text{UiO-66}_m@x$) or the corresponding shrinkage samples. These samples were then shaken at 200 rpm and 37°C . The desorbed amounts of VB were then monitored at different time intervals by UV–Vis titration. 2 ml of the desorbed solution was withdrawn for measurements and returned to the corresponding vials after the measurement.

Electrocatalysis. The catalyst ink was prepared by mixing 5 mg of active material (based on UiO-66 xerogel monoliths) and 1 mg of Vulcan XC72 carbon in a solution of isopropyl alcohol (400 μL) and Nafion (30 μL). The catalyst ink (20 and 5 μL) was coated on the GCE (area = 0.195 cm^2), which was used as the working electrode.

Section S3: Material Characterizations

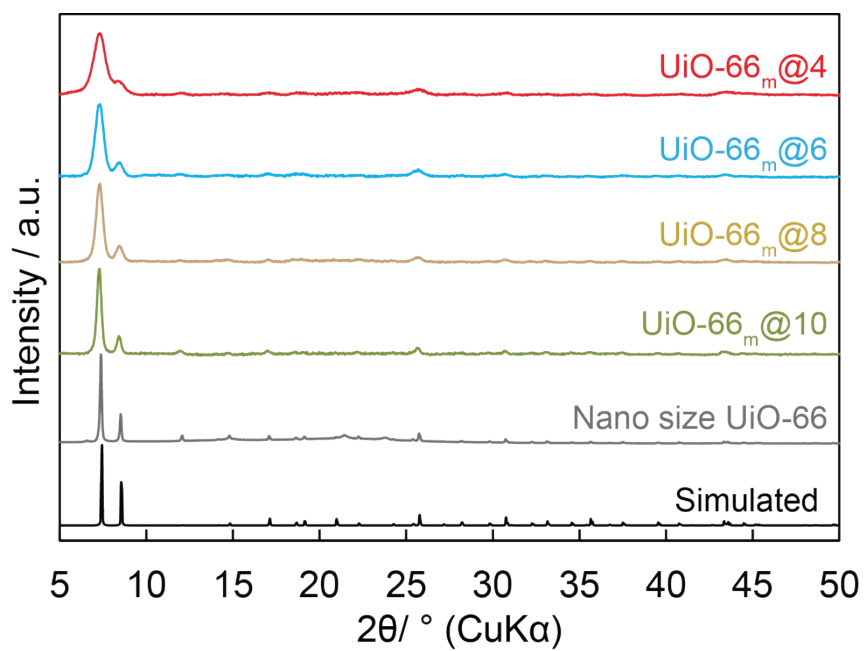


Figure S1. PXRD patterns of UiO-66 gels at different HCOOH amounts.

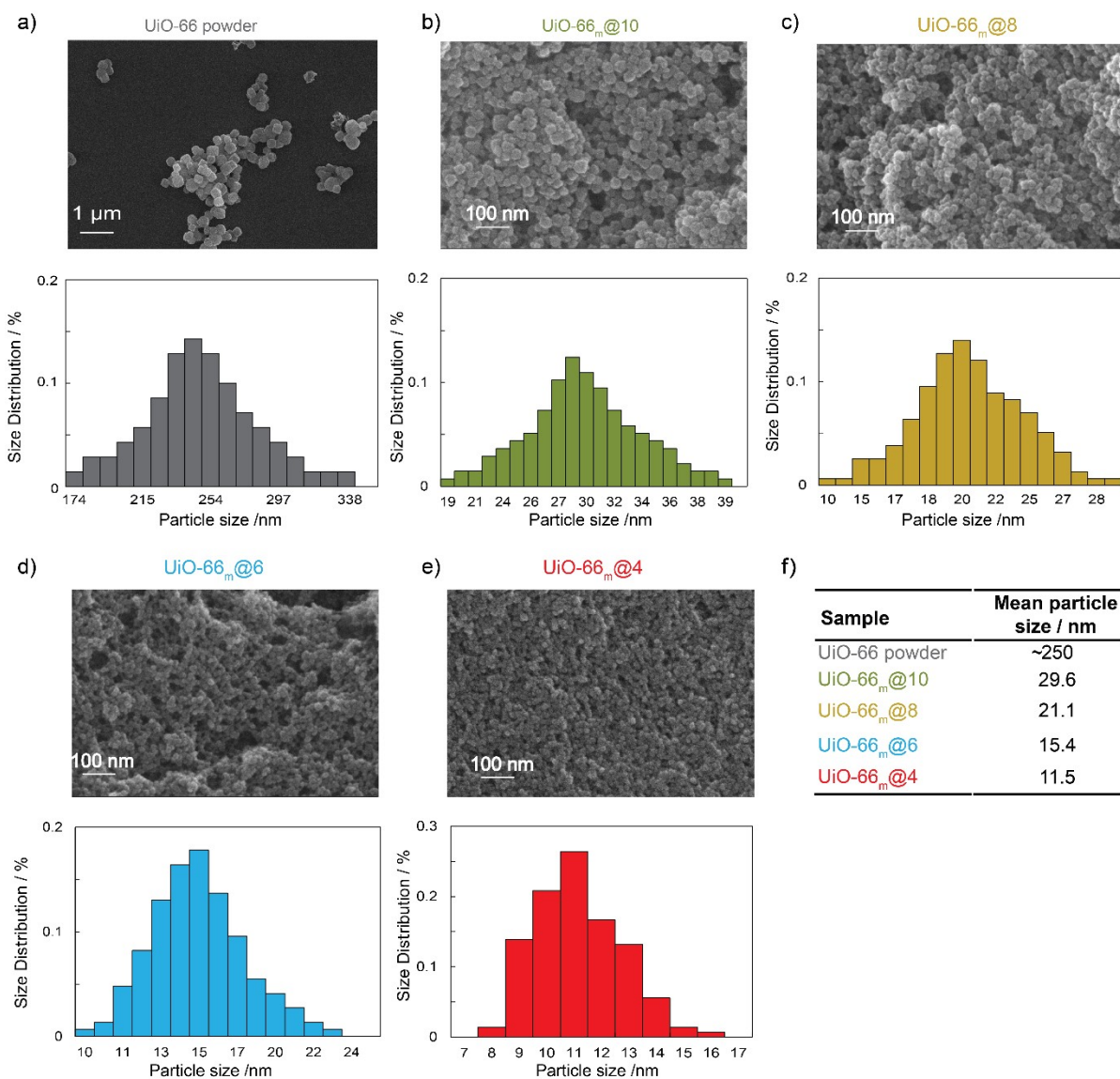


Figure S2. Scanning electron microscope (SEM) images of UiO-66 xerogel monoliths at different HCOOH amounts.

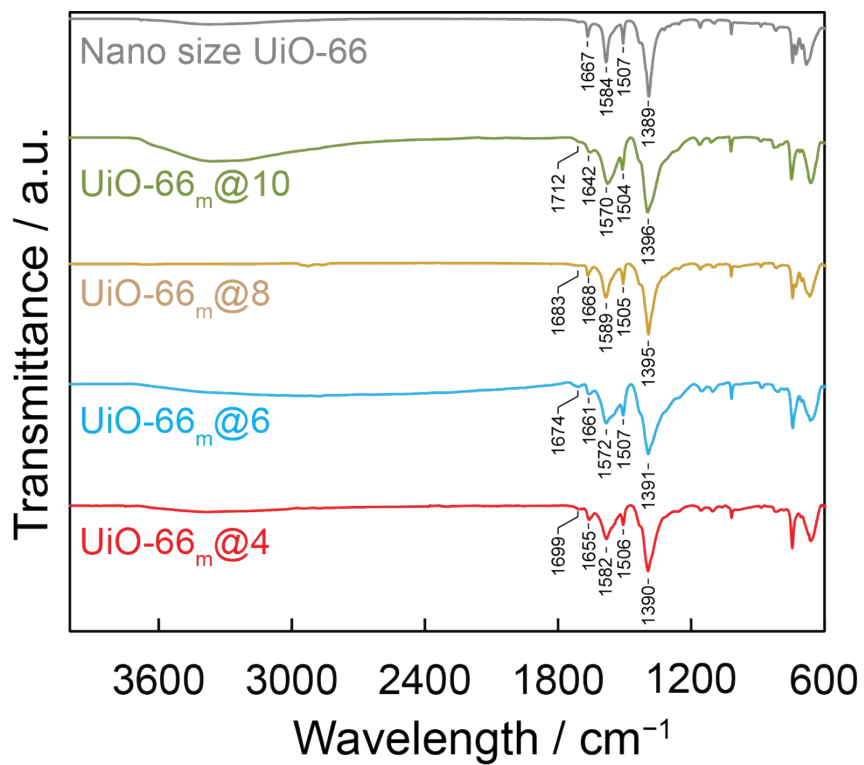


Figure S3. FT-IR spectra of UiO-66 xerogel monoliths at different HCOOH amounts.

Section S3: Vitamin B12 Adsorption and Entrapment

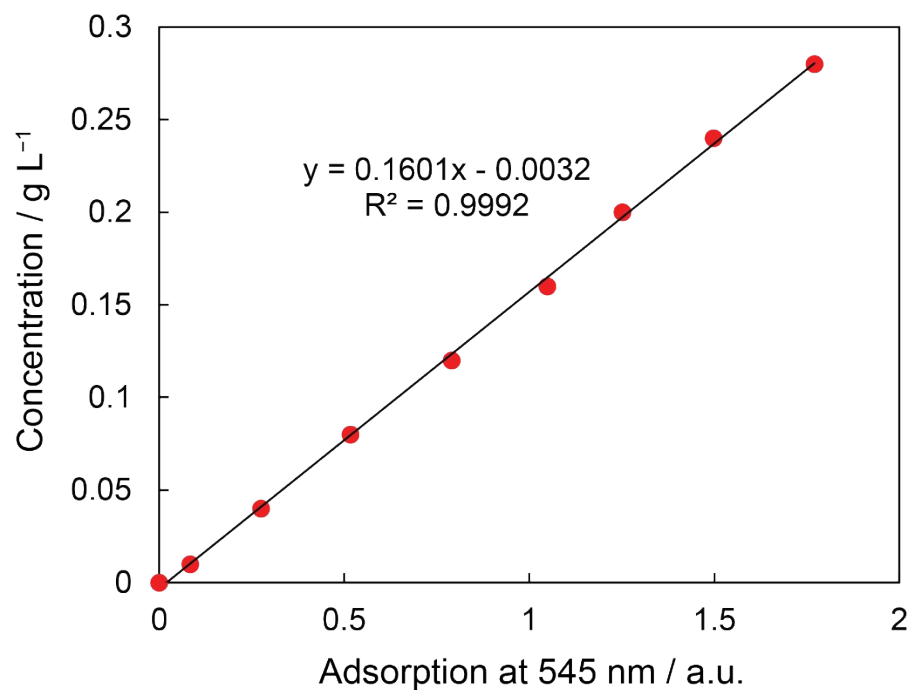


Figure S4. Standard curve for UV-Vis titration of VB in EtOH.

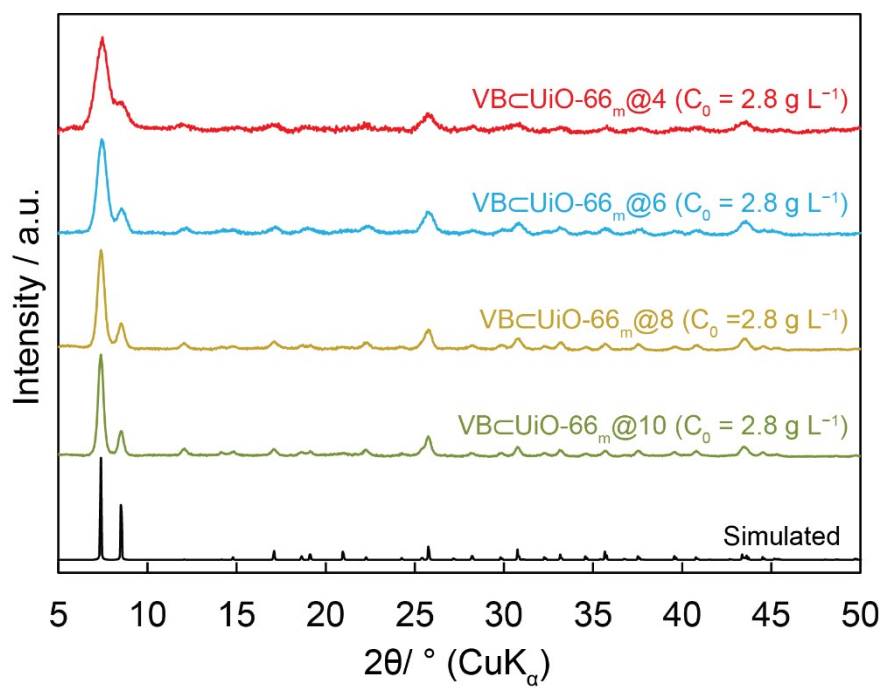


Figure S5. PXRD patterns of $\text{VBcUiO-66}_m@x$ at $C_0 = 2.8 \text{ g L}^{-1}$.

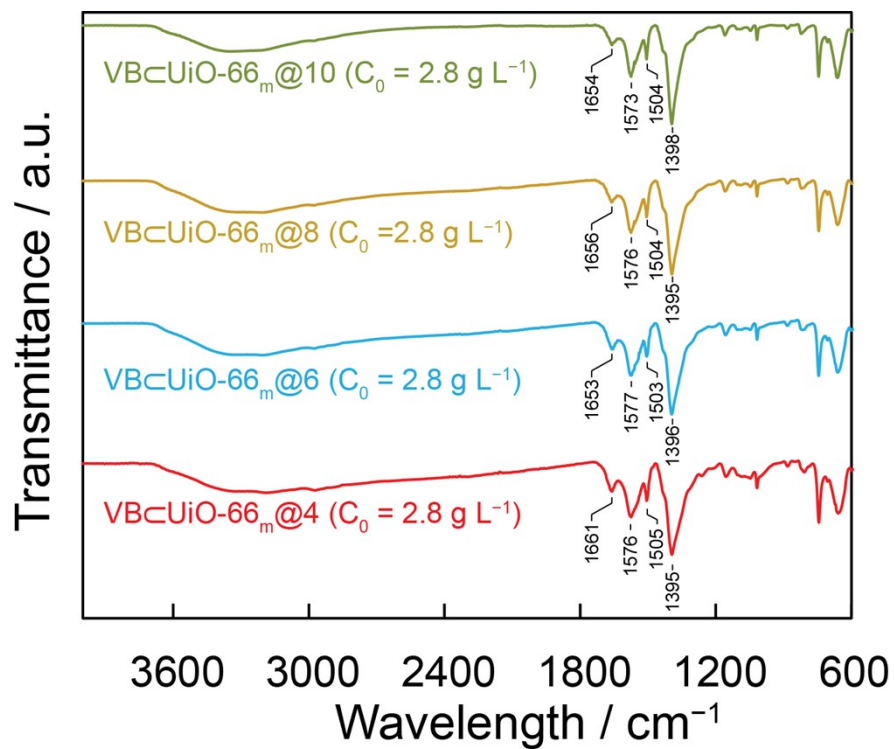


Figure S6. FT-IR spectrum of VBcUiO-66_m@x at C₀ = 2.8 g L⁻¹.

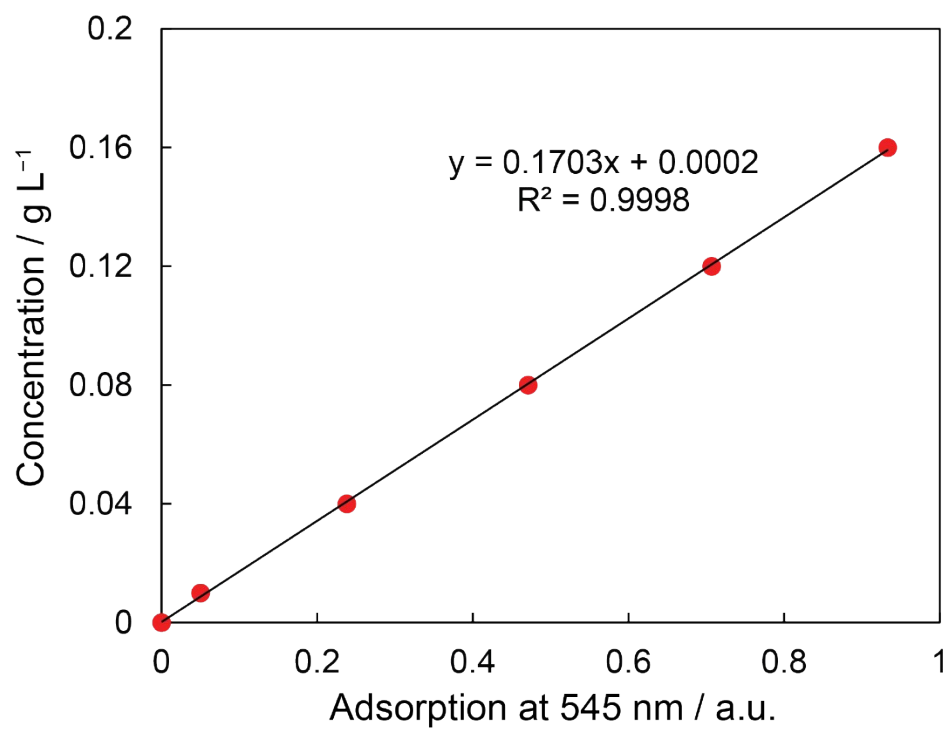


Figure S7. Standard curve for UV-Vis titration of VB in water.

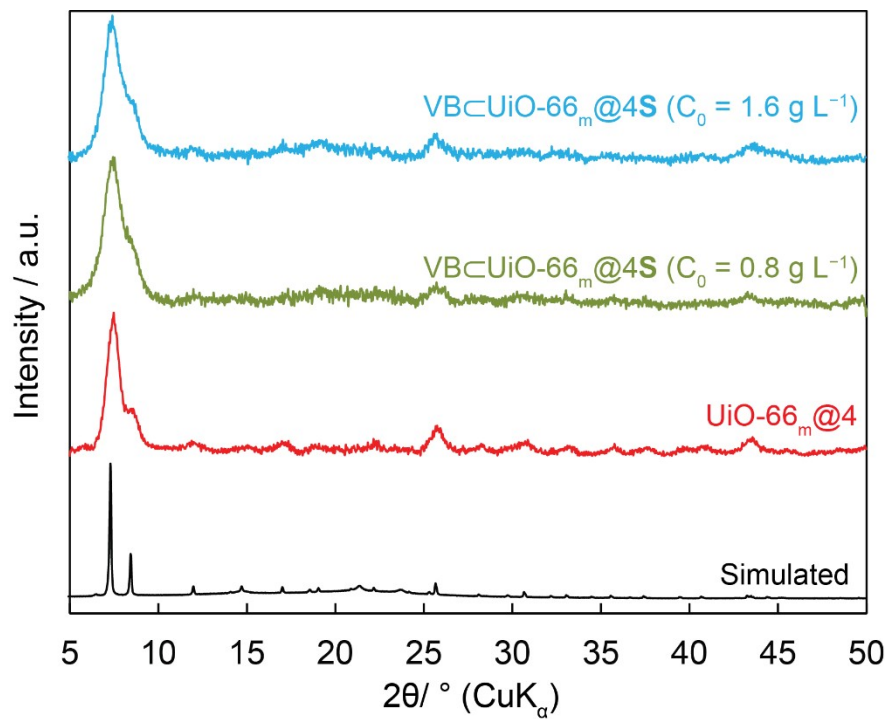


Figure S8. PXRD patterns of activated VB \subset UiO-66_m@4S at C₀ = 0.8 and 1.6 g L⁻¹ in comparison with UiO-66_m@4.

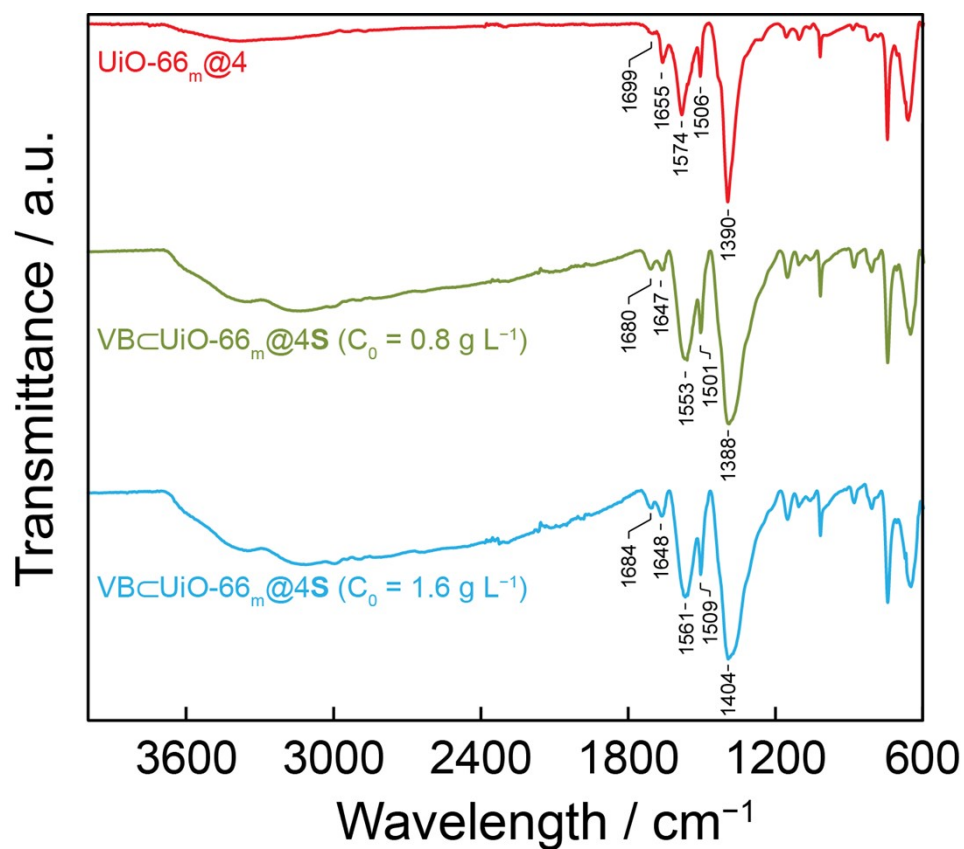


Figure S9. FT-IR spectrum of activated VBcUiO-66_m@4S at C₀ = 0.8 and 1.6 g L⁻¹ in comparison with UiO-66_m@4.

Section S4: Investigations of Hydrogen Evolution Reaction

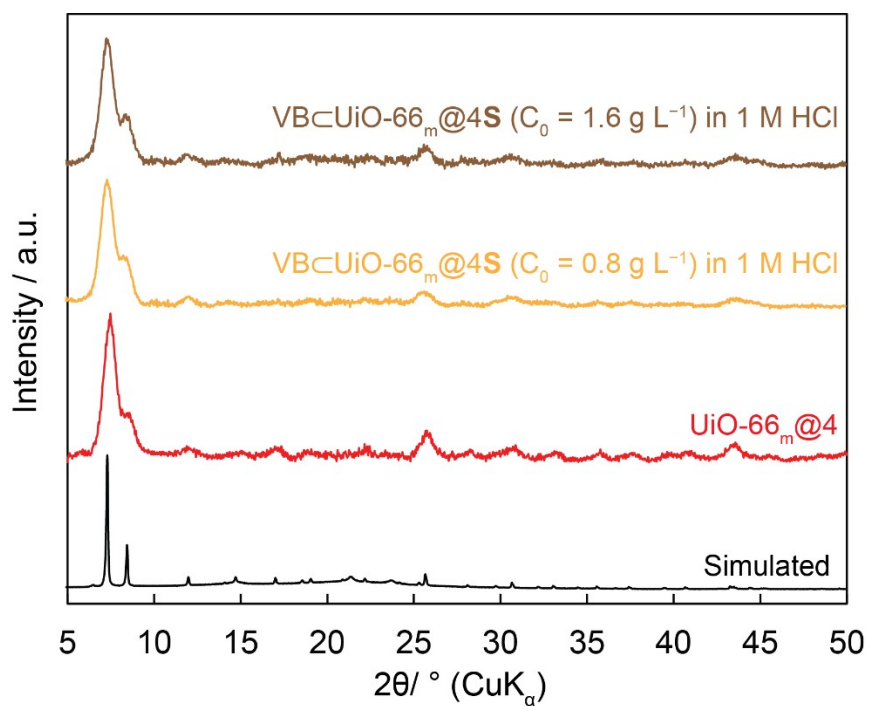


Figure S10. PXRD patterns of $\text{VBcUiO-66}_m@4\text{S}$ ($C_0 = 0.8$ and 1.6 g L^{-1}) after soaking in acidic water (1-M HCl) for 24 h compared with $\text{UiO-66}_m@4$.

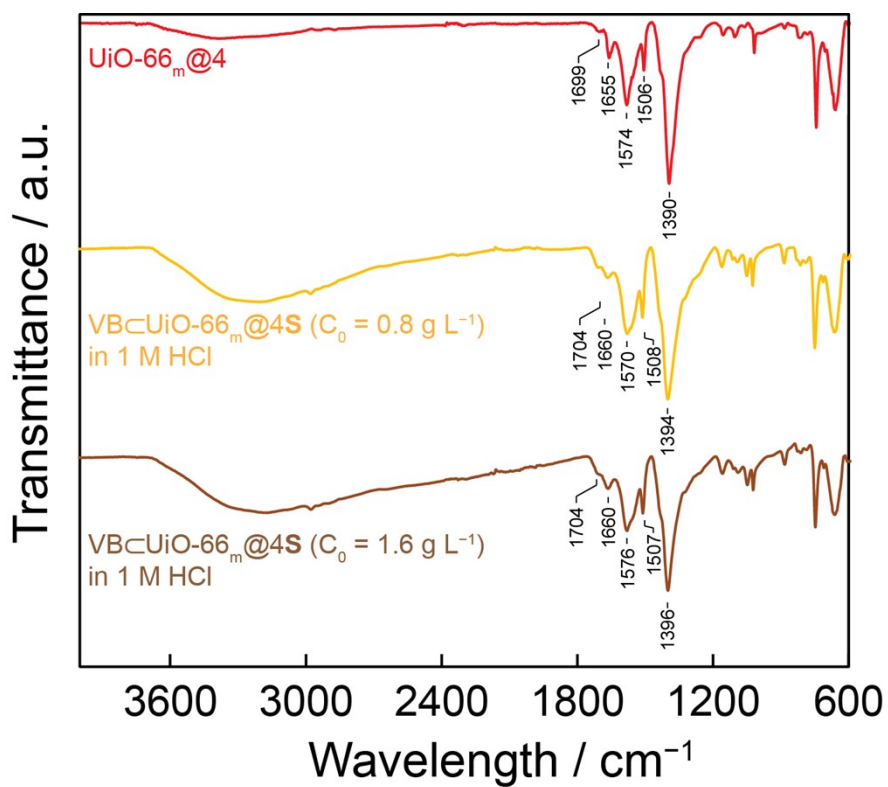


Figure S11. FT-IR spectrum of VBCUiO-66_m@4S (C₀ = 0.8 and 1.6 g L⁻¹) after soaking in acidic water (1-M HCl) for 24 h compared with UiO-66_m@4.

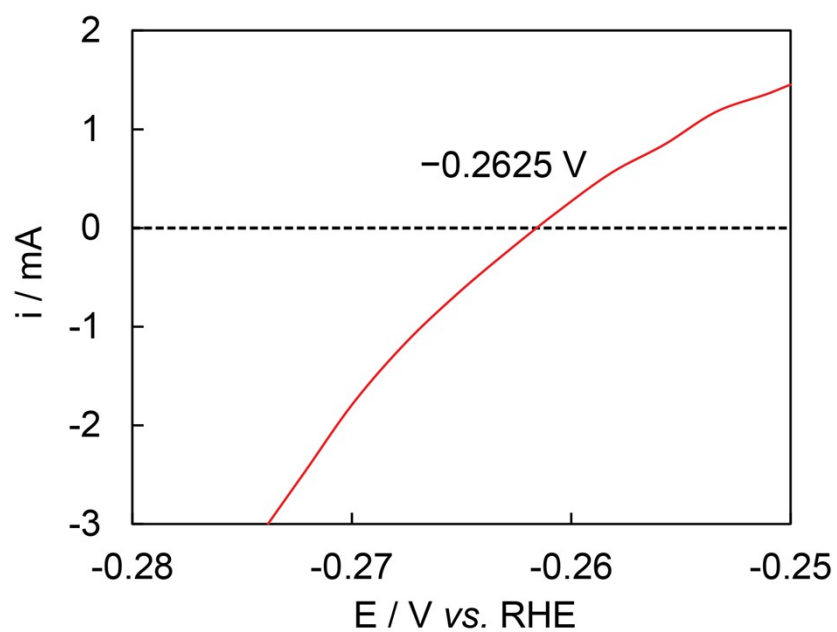


Figure S12. RHE voltage calibration under H₂-saturated 1-M HCl electrolyte. Electrodes: Pt foil: working electrodes; carbon rod: counter electrode; calomel: reference electrode.¹

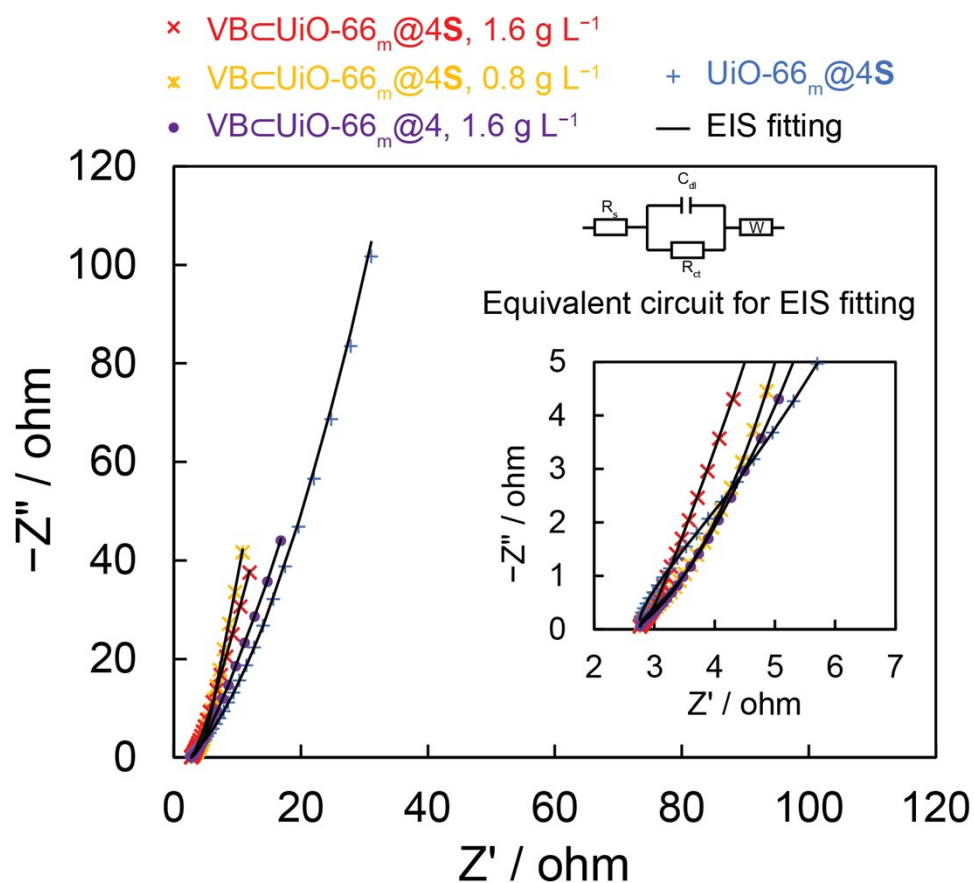


Figure S13. EIS of VB \subset UiO-66_m@4 at $C_0 = 1.6 \text{ g L}^{-1}$, VB \subset UiO-66_m@4S at $C_0 = 0.8$ and 1.6 g L^{-1} , and UiO-66_m@4S and the fitting comparison from the equivalent circuit.

Table S1. EIS fitting parameters of Nyquist plots

Sample	R_s (ohm)	R_{ct} (ohm)	W (ohm)	C_{dl} (mF)
UiO-66 _m @4S	2.76	4.252	0.0326	0.02389
VBcUiO-66 _m @4, 1.6 g L ⁻¹	2.77	0.684	0.0456	0.02142
VBcUiO-66 _m @4S, 0.8 g L ⁻¹	2.76	0.914	0.0163	0.05264
VBcUiO-66 _m @4S, 1.6 g L ⁻¹	2.76	0.551	0.0089	0.11425

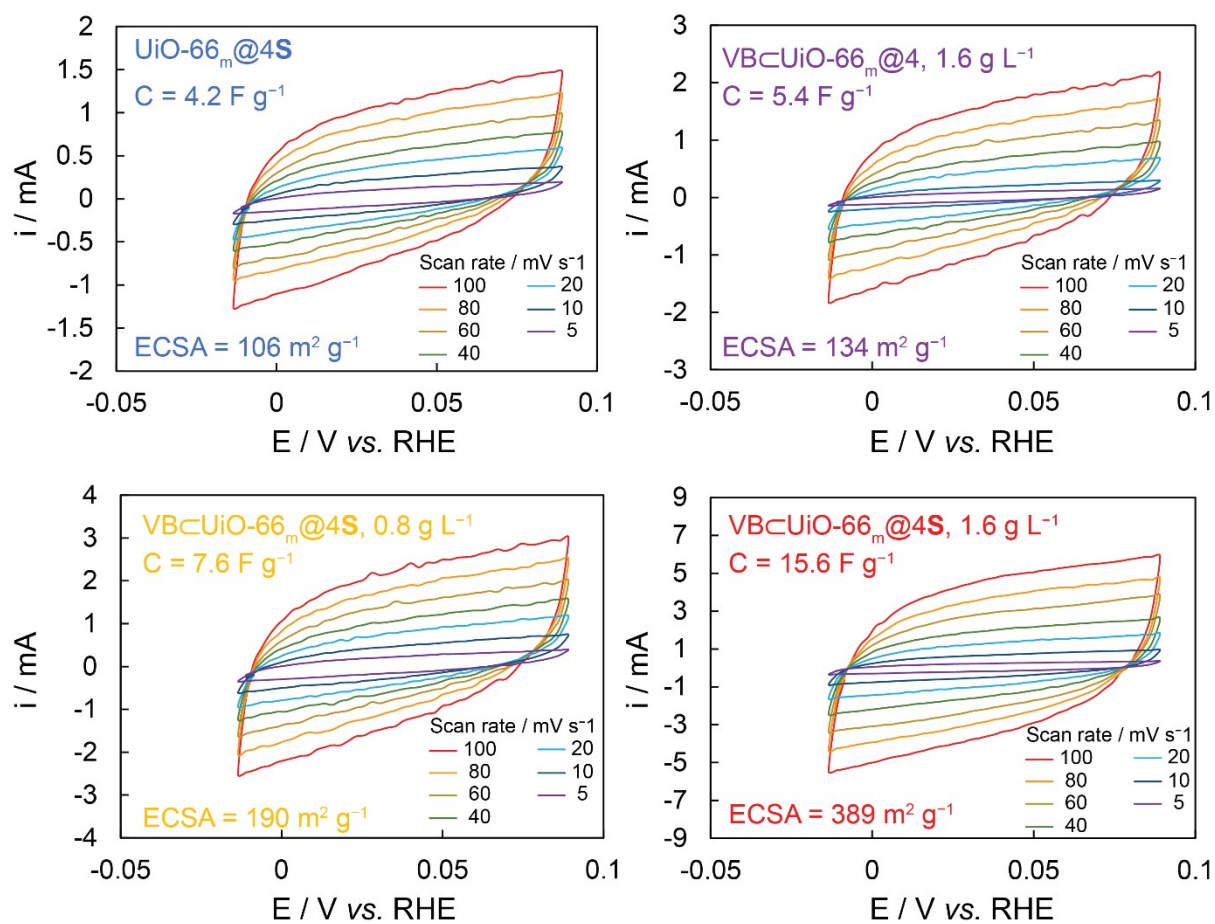


Figure S14. CV Curves and electrochemical active surface area (ECSA) of $\text{VBcUiO-66}_m@4$ at $C_0 = 1.6 \text{ g L}^{-1}$, $\text{VBcUiO-66}_m@4\text{S}$ at $C_0 = 0.8$ and 1.6 g L^{-1} , and $\text{UiO-66}_m@4\text{S}$.

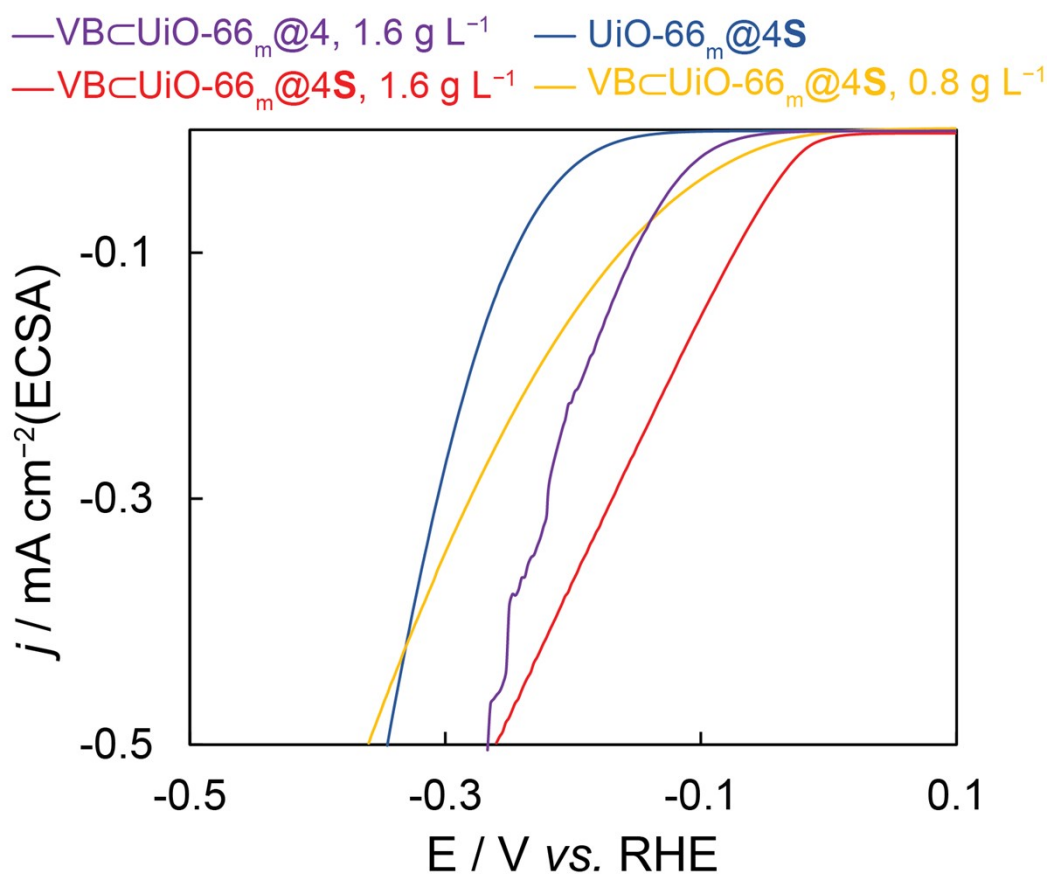


Figure S15. Normalized LSV curves (to ECSA / cm²) of VBCUiO-66_m@4 at $C_0 = 1.6$ g L⁻¹, VBCUiO-66_m@4S at $C_0 = 0.8$ and 1.6 g L⁻¹, and UiO-66_m@4S.

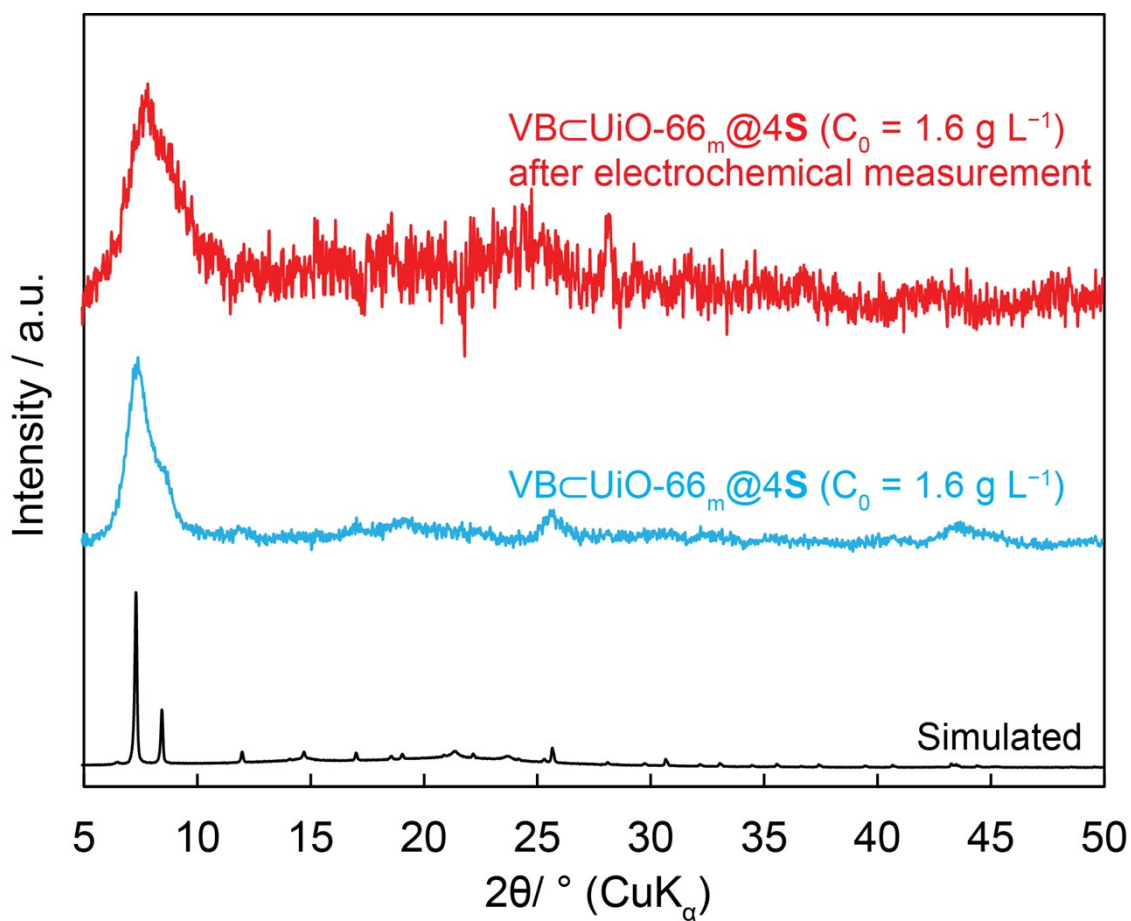


Figure S16. PXRD patterns of $\text{VB@UiO-66}_m\text{@4S}$ ($C_0 = 1.6 \text{ g L}^{-1}$) after CV cycling for 6 h in H_2 -saturated 1-M HCl electrolyte.

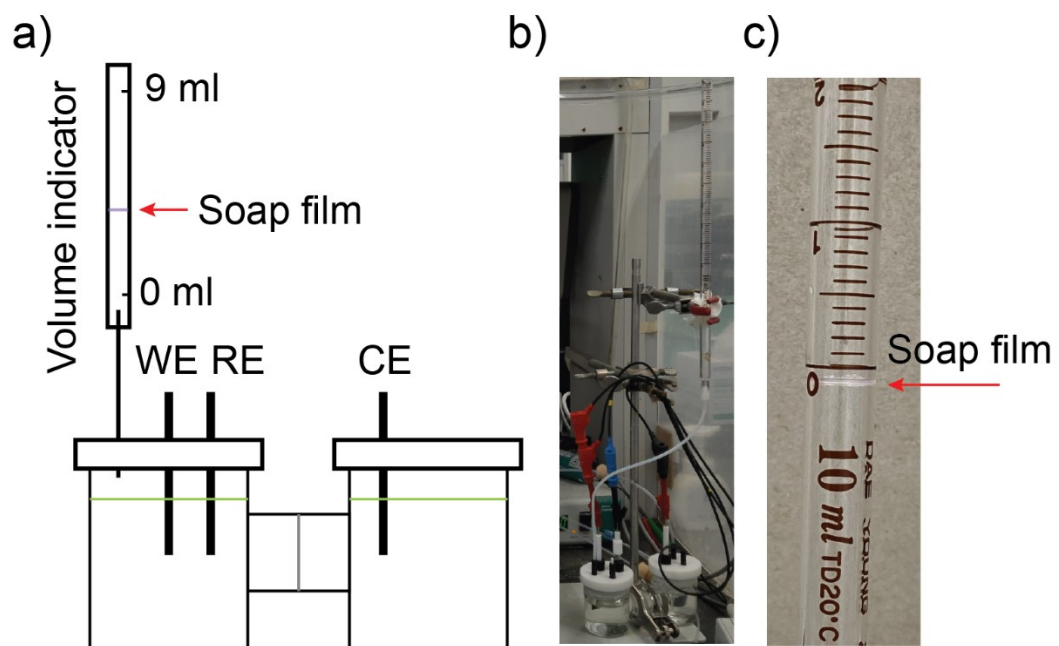


Figure S17. Setup of H-type electrolytic cell for volumetric determination of H_2 formation: a and b) H-type electrolytic cell setup; c) Soap film flowmeter.

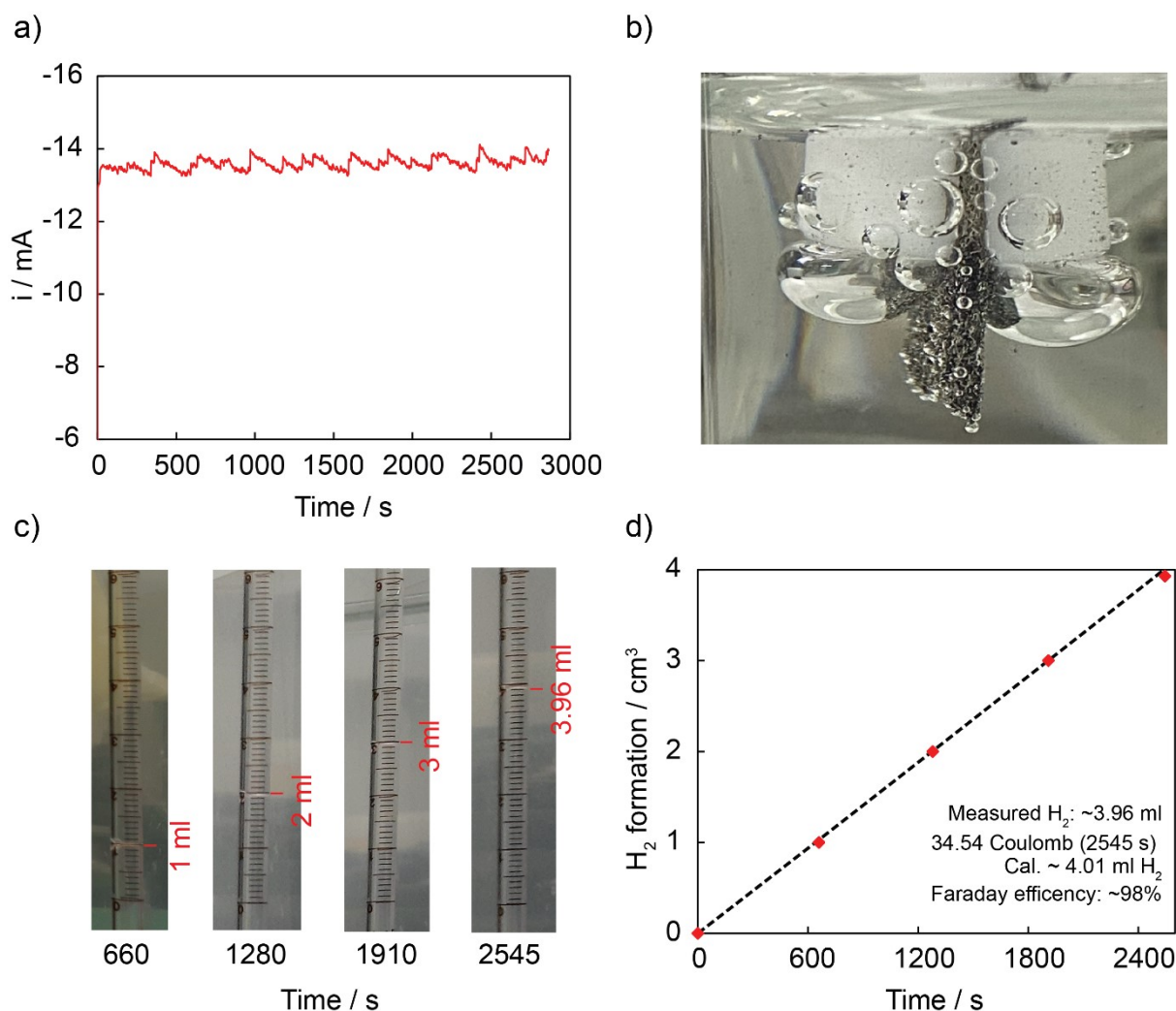


Figure S18. Volumetric determination of H_2 and calculation of faradaic efficiency: a) Chronoamperometry investigation of current vs. time; b) H_2 bubbles at working electrode; c) volumetric determination of H_2 using soap film flow meter; d) amount of hydrogen formed theoretically and experimentally. Setup: Nickel foam: working electrodes (0.45-cm^2 geometric area; $\sim 0.116\text{-mg}$ catalyst based on VB); Pt foil: counter electrode; Ag/AgCl: reference electrode. The electrolyte (1-M HCl) was saturated with H_2 before measurements.

Reference

1. Pu, Z.; Liu, T.; Zhang, G.; Chen, Z.; Li, D.S.; Chen, N.; Chen, W.; Chen, Z.; Sun, S. General Synthesis of Transition-Metal-Based Carbon-Group Intermetallic Catalysts for Efficient Electrocatalytic Hydrogen Evolution in Wide pH Range. *Adv. Energy Mater.* 2022, **12**, 2200293.
2. Anantharaj, S.; Karthik, P. E.; Noda, S. The Significance of Properly Reporting Turnover Frequency in Electrocatalysis Research. *Angew. Chem. Int. Ed.* 2021, **60**, 23051–23067.